ELSEVIER

Journal of Nuclear Materials 290–293 (2001) 1074–1078

journal of nuclear materials

www.elsevier.nl/locate/jnucmat

Macroscopic erosion of plasma facing and nearby components during plasma instabilities: the droplet shielding phenomenon

A. Hassanein *, I. Konkashbaev [1]

Argonne National Laboratory, Bldg 362, 9700 South Cass Avenue, Argonne, IL 60439, USA

Abstract

Erosion losses due to ablation during a plasma disruption can be extremely high. This can severely limit divertor system lifetime to only a few disruptions. Ablation is mass loss in the form of macroscopic particles (MPs), i.e., droplets of liquid metals or large pieces (grains or crystallites) of non-melting materials such as carbon-based materials. Results of self-consistent magnetohydrodynamic (MHD) calculations are obtained that couple the dynamics of both vapor cloud and MP interaction to incoming ions and electrons from the collisionless scrape-off layer during the disruption. The equation of motion of the MPs is solved inside the inhomogeneous vapor-cloud conditions. For a well-confined vapor cloud, the flight time of MPs in the vapor is short, and complete vaporization of the emitted MPs occurs. This will result in further reduction of net radiation power to the surface, i.e., 'droplet shielding' effect. However, if the vapor cloud has a high velocity component along the divertor surface, the MPs are quickly removed from the hot vapor region. A shorter flight time of the MPs in the vapor cloud can result in significant mass losses and extremely short erosion lifetime of the divertor surface and nearby components.

Keywords: Disruption; MHD; Erosion; Splashing; Ablation; Shielding; Lifetime; HEIGHTS package

1. Introduction

During plasma disruptions, the power flux reaching the divertor surface due to the vapor shielding effect is significantly reduced to <10% of the initial incident power flux from the scrape-off layer [1]. Mass losses from surface vaporization may be tolerated due to the reduced radiation power for a reasonable disruption frequency. However, mass losses due to ablation can be extremely high and can severely limit divertor system lifetime to only few disruptions. Ablation is mass loss in the form of macroscopic particles (MPs), i.e., droplets of liquid metals or large pieces (grains or crystallites) of non-melting materials such as carbon-based materials (CBMs). Eroded MPs will also interact with incoming plasma particles and with the vapor cloud above the surface. Therefore, the dynamic behavior of the MPs in the vapor cloud and their influence on total erosion rate is a critically important problem.

The computer simulation package HEIGHTS has been used to study in detail the different effects on target materials of the sudden high-energy deposition of various sources [2]. The HEIGHTS package consists of several integrated and self-consistent models that study dynamics of solid/liquid target evolution, MHD of vapor plasma, and evolution of MPs and their interactions with both vapor and disrupting plasmas.

This study focuses on modeling the evolution of macroscopic erosion products and their dynamic interaction with the vapor cloud. An overall examination of erosion of plasma-facing components would cover surface vaporization, macroscopic erosion from liquid–metal splashing and brittle destruction of CBMs, and erosion damage to nearby components from intense vapor radiation and deposition.

* Corresponding author. Tel.: +1-630 252 5889; fax: +1-630 252 5287.

E-mail address: hassanein@anl.gov (A. Hassanein).

[1] Permanent address: Troitsk Institute for Innovation and Fusion Research, Troitsk, Moscow Region, Russian Federation.

0022-3115/01/$ - see front matter
PII: S0022-3115(00)00665-6

2. Erosion products

The detailed vapor-cloud motion above the exposed surface is calculated by solving the vapor MHD equations for conservation of mass, momentum, and energy under the influence of a strong inclined magnetic field [3]. Because of the vapor shielding, the net erosion loss from surface vaporization in this case is only a few micrometers.

However, for liquid–metal surfaces, ablation was predicted theoretically to be in the form of macroscopic metal droplets due to splashing of the molten layer [4]. Such ablation occurs as a result of splashing of the liquid layer, mainly due to boiling and explosion of gas bubbles in the liquid, absorption of plasma momentum, and hydrodynamic instabilities developed in the liquid layer from various forces. Simulation experiments of plasma disruption have also shown that erosion of metallic materials can be much higher than mass losses caused by surface vaporization [5,6]. The mass losses are in the form of liquid droplets with average sizes of few tens of micrometers and leaving the target surface with velocity $V \approx 10$–50 m/s [5]. Hydrodynamic instabilities can occur if the vapor plasma is not well confined. Bubble formation and boiling occur from overheating of the target [3].

The ejected MPs will form a droplet cloud above the target surface and moving inside the initial vapor cloud. Photon radiation power from the upper vapor regions will be absorbed by both the target surface and a mixture of vapor and droplets above the surface. Therefore, in such a mixture of erosion products, further screening, i.e., droplet shielding of the original target surface, takes place due to MPs that have the effect of reducing photon radiation power to the target surface. Fig. 1 is a schematic illustration of MP evolution and interaction with the vapor cloud during plasma instabilities.

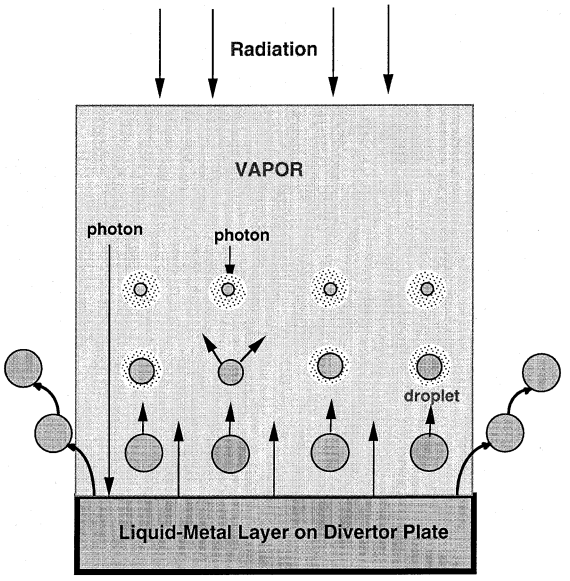

Fig. 1. Schematic illustration of droplet shielding concept during plasma instabilities.

3. Evolution of macroscopic particles

Ablation of both melting and carbon-based materials is described by splashing/destruction waves, assuming that a layer of material heated above a certain threshold energy, $Q_{\rm th}$, is removed in the form of MPs. This energy threshold for splashing is roughly equal to the sum of a thermal energy $Q_{\rm heat}$ (required to heat the liquid above a certain threshold temperature $T_{\rm th}$ including heat of fusion, $Q_{\rm f}$, for melting materials), a separation energy to remove the MPs from the surface, and a kinetic energy for the moving droplets. The separation energy of the splashed droplets is determined from the surface tension of the liquid metal. The value of $Q_{\rm th}$ is, therefore, calculated from

$$Q_{\rm th} = Q_{\rm heat} + Q_{\rm s} + Q_{\rm k}, \tag{1}$$

where

$$Q_{\rm heat} = \int_{T_0}^{T_{\rm th}} c_{\rm v}\,{\rm d}T + Q_{\rm f}\ \text{(for melting materials)}, \tag{2}$$

$$Q_{\rm s} = N_{\rm drop} 4\pi R_{\rm do}^2 \sigma, \quad N_{\rm drop} = \frac{{\rm d}m}{{\rm d}t} \Big/ \left(V_{\rm do} \frac{4}{3} \pi R_{\rm do}^3 \right), \tag{3}$$

$$Q_{\rm k} = \frac{1}{2} \rho V_{\rm do}^2, \tag{4}$$

where T_0 is initial temperature, $c_{\rm v}$ the specific heat, $Q_{\rm s}$ the energy required for droplets separation, $Q_{\rm k}$ the kinetic energy of ejected MP, $V_{\rm do}$ the ejected velocity, $R_{\rm do}$ the radius (size), $N_{\rm drop}$ the density of the ejected MP, ${\rm d}m/{\rm d}t$ the ablation rate, and σ is surface tension. For hydrodynamic instabilities, $T_{\rm th}$ is near the melting temperature $T_{\rm melt}$, while for bubble boiling, $T_{\rm th}$ is near the vaporization temperature $T_{\rm vap}$. Therefore, the threshold energy for macroscopic erosion is determined from material properties, mechanism of macroscopic destruction, and dynamics of vapor-cloud expansion above the target surface.

Ablation of CBMs due to brittle destruction has two causes, thermal stresses and macroscopic pore explosion. Brittle erosion can also be described by using the concept of a destruction wave with separation energy, $Q_{\rm s}$, defined from the binding energy of the grains/crystallites. Because the MPs are ejected as a result of the vapor pressure, P, similar to the outside pressure, $P_{\rm out}$, the velocity of MPs can be estimated from $V_{\rm do} \leqslant \sqrt{P_{\rm out}/\rho}$. For $P_{\rm out}$ of $\approx$50 atm, $V_{\rm do}$ is $\approx$50 m/s.

4. Droplet dynamics in vapor plasma

The ejected MPs are treated as separate media interacting with the surrounding inhomogeneous vapor-cloud plasma through exchange of mass, momentum, and energy. To calculate mass and energy exchange, MP vaporization is calculated by equations similar to those for vapor-cloud dynamics [1]. Mass losses and the corresponding decrease in MP radius (size) are calculated from

$$\frac{dR_d}{dt} = -\frac{\varphi_{out}}{n_d}, \tag{5}$$

$$\frac{dE_d}{dt} = W_{rad} + W_{cond} - 4\pi R_d^2 \varphi_{out}(C_v T_d + Q_f + Q_v), \tag{6}$$

where n_d and E_d are density and net energy of MP, W_{rad} and W_{cond} the radiation and conduction energy fluxes, respectively, φ_{out} the net vapor flux from MPs surface, T_d the surface temperature of MP, and Q_v is heat of vaporization. The net vapor flux from the MPs surface is defined as the difference between the vapor flux leaving the surface (corresponding to the surface temperature) and the vapor flux from the surrounding vapor cloud that condenses at the MPs surface. Because of the decreasing MP radius, the interaction of MPs with vapor can be either collisional or collisionless. The momentum conservation law has the form

$$\begin{aligned}
&\frac{dV_d}{dt} = -\frac{F_d}{m_d}, \quad \text{for } \zeta > 1 \text{ (collisional case)},\\
&\frac{dV_d}{dt} = -\frac{\rho_o}{\rho_d}(V_d - V_o)^2 \frac{G_d}{R_d}, \quad \text{for } \zeta \leqslant 1 \text{ (collisionless case)},\\
&m_d = \rho_d \frac{4}{3}\pi R_d^3, \quad \rho_d = 4\pi R_d^2 n_d, \quad F_d = 6\pi\eta R_d (V_d - V_o),
\end{aligned} \tag{7}$$

where subscript o refers to the vapor media. The collisionality condition is determined by the parameter, ζ, where $\zeta = \frac{1}{6}(V_o/V_d)(R_d/\lambda_o)$, and λ_o is vapor mean free path. For $\zeta > 1$, the Stokes formula with viscosity η_d is used while for $\zeta \leqslant 1$, the friction force is calculated assuming the interaction of freely moving vapor with spherical particles having a geometrical factor of $G_d \approx 1$. Absorption of photon radiation power by each MP is calculated by using the absorption cross-section that takes into effect geometrical screening by other MPs. The total absorption and reflection of photon radiation are summed over all emitted MPs. Influence of a magnetic field on MPs motion and dynamics is negligible; therefore the $[\mathbf{j} \times \mathbf{B}]$ force is not taken into account.

Calculations were made for different candidate materials such as Li, Be, and C. The disrupting plasma flow is assumed to consist of two particle beams, i.e., electron and ion with similar particle kinetic energy $E_{e,i} = 10$ keV and similar power $W_{e,i} = 5$ MW/cm^2; thus, total incident plasma power is $W_p = 10$ MW/cm^2. The toroidal magnetic field is assumed to be 5 T and to have a toroidal angle α of 6°.

5. Dynamics of vapor plasma

Initially, the plasma flow heats the target surface directly. The surface is vaporized and forms a vapor cloud. Soon after, the density of this vapor cloud becomes high enough to stop all incoming particles and their energy, thus transforming plasma power into photon radiation fluxes (in the positive direction away from the target), S_{out}, and toward the target surface, S_{in}. Once the target surface is heated to a temperature corresponding to the threshold energy, a destruction wave propagates inside the target, resulting in the ejection of MPs. Due to absorption of radiation by the ejected MPs, only part of radiation power, S_{tgt}, reaches the divertor surface.

The hot and less dense front of the vapor cloud expands in the normal direction with a vapor cloud velocity of ≈1 km/s. However, the front portion of the vapor does not influence the denser and colder vapor near the target surface that contains the MPs. The effective size of this front portion of the vapor cloud is determined by the absorption depth of the incoming plasma particles, particularly plasma electrons. After a transition time of few tens of μs, depending on target material, the spatial distribution of plasma parameters (such as density, temperature, and magnetic field) become quasistationary, as shown for the Be target in Fig. 2. At the front of the expanding vapor cloud the density is lowest (n[Be] $\approx 2 \times 10^{17}$ cm^{-3}) and the temperature is highest (T[Be] ≈ 28 eV). The denser and colder vapor region actually consists of two zones. The first, very near the target surface, is governed by MP vaporization; thus density is high and temperature is low

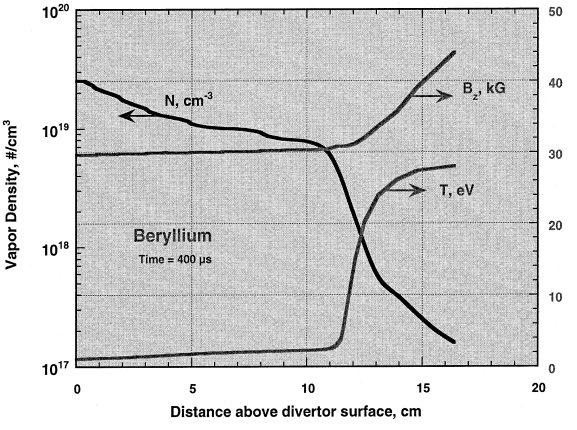

Fig. 2. Spatial evolution of Be vapor temperature, density, and toroidal magnetic field during a disruption.

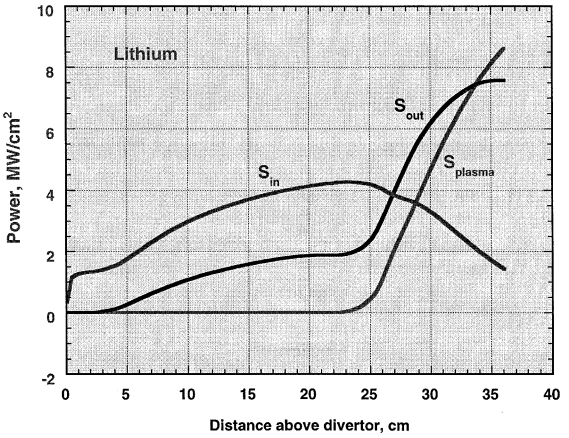

Fig. 3. Spatial distribution of emitted radiation and deposited plasma power in Li vapor.

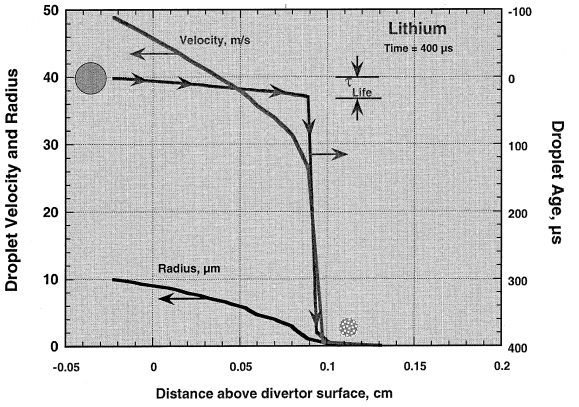

Fig. 4. Spatial evolution and lifetime of Li droplet as it moves in vapor cloud.

($T \approx 0.3$–0.5 eV). This means that the vapor is mostly neutral ($Z < 0.5$) in this zone. The second zone consists of vapor plasma with $Z \approx 1$ and is characterized by low or negligible radiation. The little radiation absorbed by some free electrons is enough to keep the vapor at this temperature. Most of this radiation, S_{in}, is absorbed by MPs near the target surface. The flowing vapor from the target surface pushes upward the magnetic field, therefore, the field in the vapor cloud is decreased to $B_z \approx 3$ T in Be vapor. Thus, the inclination angle of magnetic field lines in vapor cloud changes from $\alpha_o = 6°$ to $\alpha \approx 20°$.

Fig. 3 shows the spatial distribution of deposited plasma power (S_{plasma}), upward radiation flux (S_{out}), and downward radiation flux (S_{in}) toward the target. The plasma-particle energy is absorbed mainly by the free electrons of the vapor at high temperature and high Z and by the inner shell electrons at lower Z. It can be seen that the upward radiation is generated in this region. However, the radiation power toward the target surface, S_{in}, is absorbed mainly by vapor plasma with a lower $Z \approx 1$. For Li, the size of the radiative region is similar to the size of the zone where incoming plasma flux is absorbed. For higher-Z materials such as Be and C, radiation heat conduction is high enough to keep part of the vapor plasma outside the absorption zone at a higher temperature. Absorption of radiation ceases at temperatures lower than the ionization temperature. Near the wall, the second zone of the cold region contains MPs that can absorb radiation; thus, a sharp decrease in S_{in} occurs as shown in Fig. 3.

6. Interaction of MPs with vapor plasma

The ejected MPs move across the cold dense vapor with a maximum velocity at ejection, $V_{do} < 100$ m/s, determined from the vapor pressure above the target surface. Nevertheless, the MPs are slowed because the vapor velocity nearby the target surface is less than V_{do}. Fig. 4 shows the spatial evolution of a Li droplet with an initial radius of 10 μm and a velocity of 50 m/s as it moves across the Li vapor cloud at time equal to 400 μs. The Li droplet is completely vaporized at distance $\lambda_{Li} \approx 1$ mm above the target with a lifetime, $\tau_{life} \approx 40$ μs in the vapor cloud. The 'birth time', i.e., time when the particle/droplet was ejected is also shown. The earlier-born MPs were moved farther from the target surface for a longer time. A beryllium droplet travels much farther than a Li droplet ($\lambda_{Be} \approx 10\lambda_{Li}$) because of its higher vaporization energy and lower radiation power at the droplet surface ($S_{tgt}(Be) \approx 230$ kW/cm^2 versus $S_{tgt}(Li) \approx 300$ kW/cm^2). MP lifetime is determined by the incoming radiation power and vaporization energy; thus $\tau_{life}(Li) \approx 40$ μs, but $\tau_{life}(Be) \approx 240$ μs, and $\tau_{life}(C) > 400$ μs.

The calculations were repeated for different initial values of R_{do} (3–100 μm) and V_{do} (10–200 m/s). It is interesting to conclude that the dependence of the erosion rate on the initial droplet size and velocity is very small. The size and velocity of the droplets have influence only on the distance, λ, that these droplets travel before complete burning. In most studied cases, however, $\lambda \approx 1$–2 cm that is much less than the size of the vapor-cloud ≈20–30 cm. In the case of not well-confined vapor plasma or different splashing mechanisms some MPs can have flight time less than the time for complete burning. In such a situation the size and the velocity of the MPs can play a more important role. However, the erosion rate is very high in this case [3].

In examining mechanism and dynamics of the splashing/destruction wave, we can see that during the initial phase, the target surface is heated by both plasma particles and photon radiation while the surface temperature is achieving the threshold temperature/energy. Then a splashing wave propagates into the target bulk.

The front wave position x_{wave} inside the target is determined by the threshold condition $T(x_{wave}) = T_{th}$. All target mass behind the wave front with $x < x_{wave}$ is emitted as MPs. Depending on material properties and the mechanism of splashing/brittle destruction, these MPs have a certain distribution in size R_{do}, velocities V_{do}, and angles of ejection. The calculations have also shown that the initial distribution of MP sizes and velocities does not affect the net radiation power to the target surface, only the vaporization path length of the MPs as mentioned above.

The process of ablation mass losses can be divided into two stages. In the first stage, the splashing wave propagates quickly because the target surface is heated near T_{th} at sufficient depth and any slight additional radiation power is enough to achieve threshold conditions. Therefore, sufficient mass is ejected in a short time, and both mass and duration are determined by material properties. The time evolution of a Be target surface temperature, T_s, and droplet and total vapor mass losses is shown in Fig. 5. The time history of splashing erosion waves of Be droplets are shown. Similar to the vapor-cloud front temperature T_v, the target surface temperature also achieves a quasistationary value after a certain duration time. After the first ejection wave, the process has a quasistationary form in which the flux of ejected MPs becomes equal to the flux of disappearing MPs. For a Li target, this state is quickly achieved (in <20 μs), but for materials with higher T_{vap} such as Be, this state requires the much longer time of $\approx$150 μs. For materials with even higher T_{vap}, such as CBMs, such a state was not achieved even after 600 μs. Total mass loss is therefore determined from the net radiation flux arriving at the target surface after the double-shielding effect due to absorption by both vapor plasma and MPs. The vapor and droplet shielding efficiency is $>95\%$ for the candidate materials and the conditions studied in this analysis.

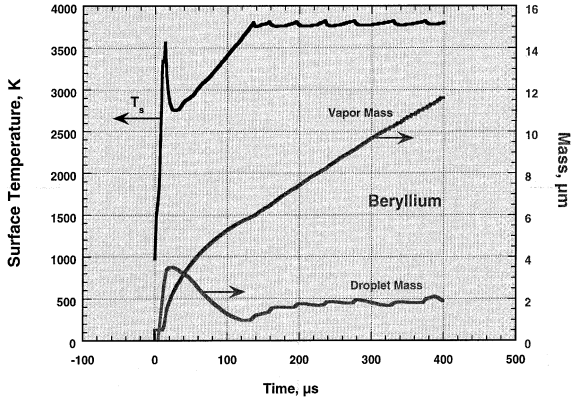

Fig. 5. Time evolution of Be target surface temperature, droplet mass, and total vapor mass.

7. Summary and conclusions

Two separate mechanisms of material erosion occur during plasma disruptions: vaporization from the target surface and ablation in the form of macroscopic particles (MPs which are liquid metal droplets or macroscopic pieces of carbon-based materials). Ablation can occur due to several mechanisms; hydrodynamic instabilities, volume bubble boiling (metallic materials), and thermal stresses and pore explosion (brittle materials). Numerical simulation using the HEIGHTS computer package was carried out by using new models for dynamic evolution and interaction of MPs with the inhomogeneous vapor cloud. The ablation mechanism plays the more important role because the required threshold energy needed for ablation is much less than the energy of vaporization. Ablation can result in significant mass losses if the ejected MPs are removed quickly before they are completely vaporized. In the absence of strong plasma and vapor wind or vapor turbulent diffusion, a new process called 'droplet shielding' occurs, resulting in significantly reduced total mass losses from the target surface. The shielding efficiency of both vapor and droplet shielding in a well-confined vapor plasma can exceed 95% for candidate materials such as Li, Be, and C. For a typical disruption time in an ITER-like machine of $\tau \approx 1$ ms, the predicted mass losses per disruption are $X_{loss}(\mathrm{Li}) \approx 750$ μm, $X_{loss}(\mathrm{Be}) \approx 30$ μm, and $X_{loss}(\mathrm{C}) \approx 22$ μm. These values may seem acceptable from an engineering standpoint, but one should note that the foregoing analysis assumed no vapor/plasma wind or turbulence diffusion along the divertor plate surface. In such a case, the actual erosion values of divertor plate and nearby components will be significantly increased. In addition, redeposition of eroded and splashed materials on reactor components can adversely affect plasma performance.

Acknowledgements

This work is partially supported by the U.S. Department of Energy, Office of Fusion Energy Science, under Contract W-31-109-Eng-38.

References

[1] A. Hassanein, Fus. Technol. 30 (1996) 713.
[2] A. Hassanein, I. Konkashbaev, J. Nucl. Mater. 273 (1999) 326.
[3] A. Hassanein, I. Konkashbaev, J. Nucl. Mater. 283–287 (2000) 1171.
[4] A. Hassanein, I. Konkashbaev, Suppl. J. Nucl. Fus. 5 (1994) 193.
[5] V. Belan et al., J. Nucl. Mater. 233–237 (1996) 763.
[6] N.I. Arkhipov et al., J. Nucl. Mater. 233–237 (1996) 767.